

Biodegradable and Flexible Polymer Based Memristor Possessing Optimized Synaptic Plasticity for Eco-Friendly Wearable Neural Networks with High Energy Efficiency

Sungjun Oh¹, Hyungjin Kim¹, Seong Eun Kim¹, Min-Hwi Kim¹, Hea-Lim Park¹, and Sin-Hyung Lee¹

¹Affiliation not available

October 17, 2022

Abstract

Organic memristors are promising candidates for the flexible synaptic components of wearable intelligent systems. With heightened concerns for the environment, considerable effort has been made to develop organic transient memristors to realize eco-friendly flexible neural networks. However, in the transient neural networks, achieving flexible memristors with bio-realistic synaptic plasticity for energy efficient learning processes is still challenging. Here, we demonstrate a biodegradable and flexible polymer based memristor, suitable for the spike-dependent learning process. An electrochemical metallization phenomenon for the conductive nanofilament growth in a polymer medium of poly (vinyl alcohol) (PVA) is analyzed and a PVA based transient and flexible artificial synapse is developed. The developed device exhibits superior biodegradability and stable mechanical flexibility due to the high water solubility and excellent tensile strength of the PVA film, respectively. In addition, the developed flexible memristor is operated as a reliable synaptic device with optimized synaptic plasticity, which is ideal for artificial neural networks with the spike-dependent operations. The developed device is found to be effectively served as a reliable synaptic component with high energy efficiency in practical neural networks. This novel strategy for developing transient and flexible artificial synapses can be a fundamental platform for realizing eco-friendly wearable intelligent systems.

Corresponding author(s) Email: sinhlee@knu.ac.kr

ToC Figure

Transient Flexible Memristor

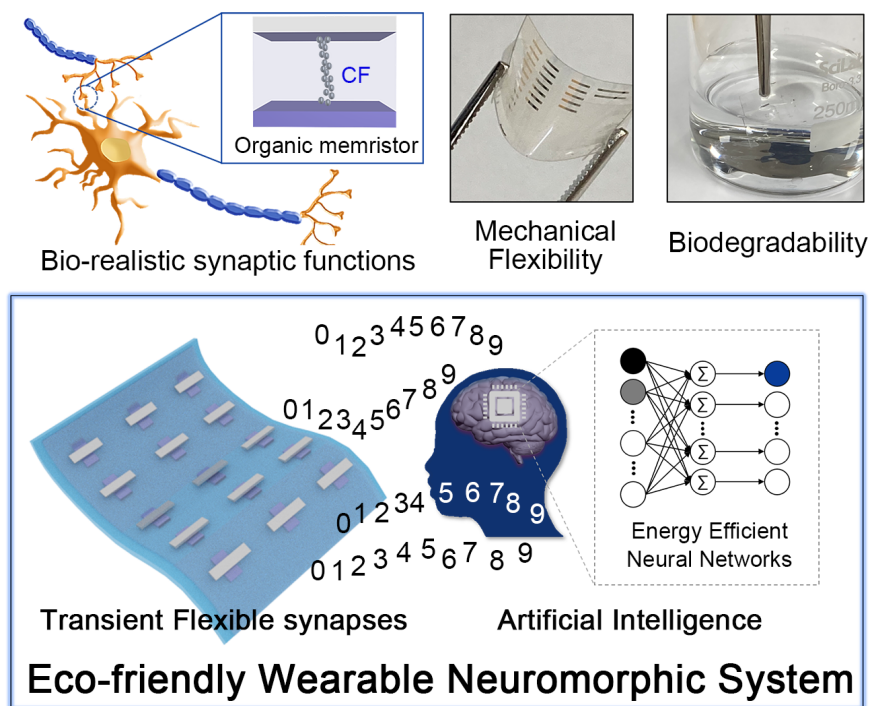


Figure 1: **ToC Figure.** A biodegradable and flexible polymer based memristor for eco-friendly artificial synapses is demonstrated. The developed device exhibits superior biodegradability and mechanical flexibility due to the high water solubility and excellent tensile strength of the polymer, respectively. Moreover, the memristors are operated as reliable synaptic cells with optimized synaptic plasticity, which is ideal for artificial neural networks with high energy efficiency.

Introduction

Flexible neuromorphic electronics for the computing systems of smart wearable electronics have attracted great attention because of their merits in terms of energy efficiency and operating speed (van de Burgt et al., 2018; Feng et al., 2019; Kim et al., 2021a). In practical hardware neural networks, a memory device completely mimicking a biological synapse is a crucial component in achieving energy-efficient operations (van de Burgt et al., 2018; Lequeux et al., 2016; Sun et al., 2021; Bannur et al., 2022). An organic material based resistive switching device, i.e., an organic memristor, has been considered as a favorable memory component of flexible neuromorphic systems, in the viewpoints of mechanical flexibility and synaptic functionality (Kim et al., 2021a; Park et al., 2019; Lee et al., 2020b; Park and Lee, 2021). Thus far, diverse mechanisms for the resistive switching of organic memristors have been explored, such as ion migration (Raeis-Hosseini et al., 2018), ferroelectricity (Lu et al., 2020), and electrochemical metallization (ECM) (Kim et al., 2021a; Lee et al., 2019a; Jang et al., 2019; Park et al., 2020b). Among the various types of organic memristors, ECM-based devices have been demonstrated as promising artificial synapses of practical systems owing to their great scalability and superior electrical characteristics (Jang et al., 2019; Park et al., 2020b). For organic ECM memristors, a nanoscale metallic conductive filament (CF) is formed or ruptured in an organic medium under an electric stimulus, resulting in the resistive switching characteristics of such devices. Because the CF growth is mainly governed by the distribution of the electric field in an ECM memristor, the multilevel resistance states can be obtained by controlling the conditions of the electric stimulus (Kim et al., 2021a;

Jang et al., 2019). In addition, the stability of the CF is dependent on its structure, and thus, short-term plasticity (STP) and long-term plasticity (LTP) of biological synapses can be mimicked in the ECM device by precisely controlling the CF dynamics (Wang et al., 2016b; Hua et al., 2019). Recently, the development of transient electronics with biodegradable and biocompatible characteristics has been urgently needed as environmental concerns increased (Fu et al., 2016; Gao et al., 2017). To realize the eco-friendly practical neuromorphic systems with high energy efficiency, it is important to achieve the spike-dependent learning process in the transient artificial synapse. For such operations, the synaptic device with bio-realistic synaptic plasticity is an essential component. Specifically, the artificial synapse should possess the STP and LTP characteristics for training on different time scales of successive electric stimuli through a combination of STP and LTP (Sarwat et al., 2022). Additionally, for compatibility with other neuromorphic components, the diverse time windows for synaptic plasticity should be obtained in the synapse devices (Lee et al., 2020b). Although several studies on the biomaterial based ECM memristors with transient features have been conducted (Hosseini and Lee, 2015; He et al., 2016; Wang et al., 2016a; Wu et al., 2016; Sun et al., 2018; Song et al., 2018; Ji et al., 2018; Xu et al., 2018; Lin et al., 2019; Guo et al., 2020; Sueoka and Zhao, 2022), it is still challenging to achieve bio-realistic synaptic devices with biodegradability and flexibility, due to the difficulties in controlling the CF dynamics.

Poly(vinyl alcohol) (PVA) with high water solubility is a promising polymer for biodegradable films (Dorigato and Pegoretti, 2011; Ahmed and Hashim, 2020). It is widely utilized as an insulator in flexible electronics because of its excellent mechanical flexibility and superior electrical characterizations (Zhang et al., 2020; Wang et al., 2022). Despite such functionalities of PVA for transient and flexible electronics, the ECM phenomenon, essential for the CF growth, has not been reported in the pure PVA medium yet. Previously, PVA has not been regarded as a medium, suitable for the ECM memristor, and it has been used as an insulator for the memristors based on the ion migration (Hmar, 2018; Kim et al., 2019b; Nguyen et al., 2020) or the dipole alignment (Lei et al., 2014), and a matrix of an ion-doped electrolyte (Krishnan et al., 2018). In such devices, only the limited synaptic function (STP or LTP) was demonstrated owing to the inherent characteristics in the switching mechanism (see Table S1). Specifically, for the CF based memristor consisting of the ion-doped PVA matrix, the constant ion density restricted the synaptic function to LTP (Krishnan et al., 2018). In the memristors based on the ion-doped electrolytes, it is difficult to achieve both the LTP and STP functions because the metal ion density is governed by the doping concentration, not the electric stimuli applied to the devices (Park and Lee, 2020; Woo et al., 2021). For realizing the eco-friendly wearable neural networks with high energy efficiency, it is important to develop the transient ECM memristor with mechanical flexibility and optimized synaptic plasticity for the spike-dependent learning.

In this work, we developed a PVA-based ECM memristor with optimized synaptic plasticity for a transient artificial synapse of an eco-friendly flexible neural network with high energy efficiency, as shown in Figure 1a. The resistive switching effects attributed to the metallic CF formation in the PVA media with different molecular weights (M_w) were analyzed. When the M_w value of the polymer medium is sufficiently low, the resistive switching behaviors based on the ECM phenomenon were effectively achieved, and the memory stability and time windows for synaptic plasticity were found to be effectively tuned by the polymer M_w . On the basis of the understanding of the ECM phenomenon in the polymer medium of PVA, we fabricated a PVA-based flexible memristor with biodegradable characteristics and optimized its synaptic plasticity. The developed memristor exhibited stable nonvolatile memory characteristics during successive mechanical stresses, and it was swiftly dissolved in deionized (DI) water. Moreover, synaptic characteristics for neuromorphic systems including STP, LTP, paired-pulse facilitation (PPF), spike-number-dependent plasticity (SNDP), and spike-rate-dependent plasticity (SRDP) were successfully demonstrated in the developed device. The hardware neural networks based on the device showed the reliable logic operations with high energy efficiency. In the SPICE simulation, the device showed the great potentials for realizing practical artificial neural networks.

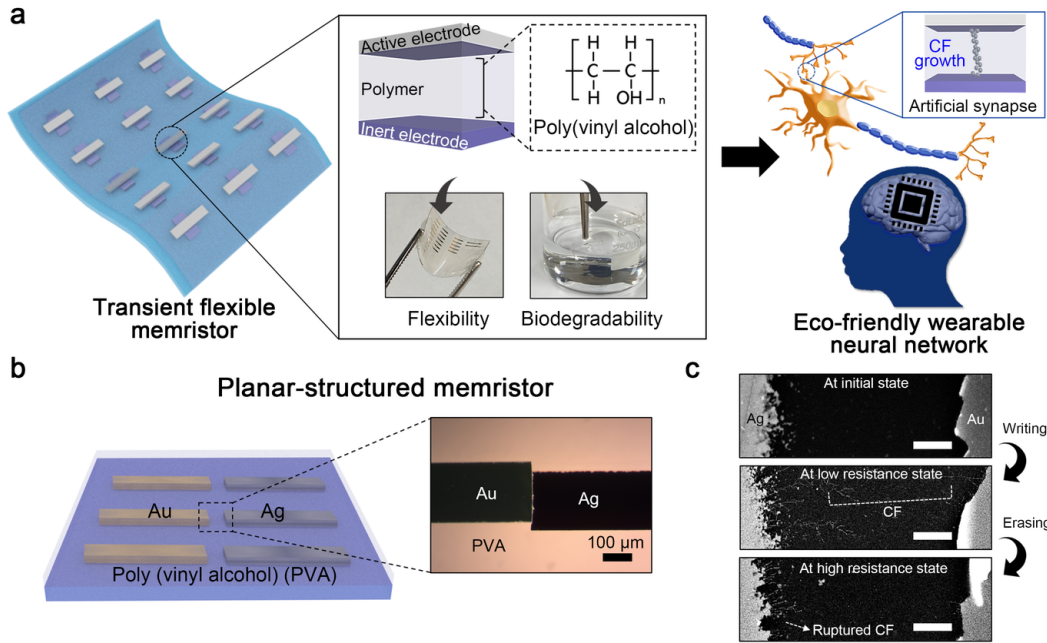


Figure 2: **Figure 1.** Dynamics of the metallic conductive filament growth in the poly(vinyl alcohol) (PVA) based memristor. (a) Schematics presenting the structure of the PVA based memristor with mechanical flexibility and biodegradability, and its potentials as an artificial synapse for hardware-based eco-friendly neural networks. (b) A schematic showing the PVA based memristors with a planar structure. Three types of the devices with the different polymer molecular weights (M_w s) (130000 , 23000 , and 10000 gmol^{-1}) were prepared. An inset image shows a microscopic photograph of the device. (c) Active surfaces of the device according to the resistance states. Each surface was investigated using a field-emission scanning electron microscope (scale bar, $1 \mu\text{m}$).

Experimental Section/Methods

The film thickness of the device was measured using a profiler (DektakXT-A, Bruker). The electrical characteristics of the devices were measured using a semiconductor parameter analyzer (4200-SCS, Keithley) combined with an ultrafast $I-V$ module (4225-PMU, Keithley), in an ambient condition with a relative humidity of 30 %, at $27 \text{ }^\circ\text{C}$. In the electrical measurements, the inert electrode (gold or indium tin oxide) was grounded, and the active electrode of silver was used for the scanning voltage. The active area of the lateral-type memristor was investigated using a field-emission scanning electron microscope (S-4800, Hitachi).

To fabricate an organic memristor with a planar structure, a glass substrate was cleaned under ultrasonication in acetone, isopropyl alcohol, and deionized water in sequence for 10 min. For the inert electrode, a 50-nm-thick gold layer was thermally deposited on the substrate at $1 \text{ } \text{\AA}/\text{s}$ under 10^{-6} Torr. The inert electrode was patterned using a photoresist (PR) (AZ 1512, AZ electronic materials) through conventional photolithography and a wet-etching process using an etchant (TFA, Transene) for gold. Then, the active electrode of 50-nm-thick silver was thermally evaporated on the PR patterned film at $1 \text{ } \text{\AA}/\text{s}$ under 10^{-6} Torr. Through the lift-off process for removing the PR, the active electrode was patterned. The width of each electrode and the gap distance between the electrodes were about 300 and $5 \mu\text{m}$, respectively. As the polymer medium, a poly(vinyl alcohol) (PVA) powder with molecular weight (M_w) of 10000, 23000, or 130000 gmol^{-1} , dissolved in deionized water in 5, 4, or 2wt%, respectively, was spin-coated on the substrate with the electrode patterns, at a rate of 2000 rpm for 30 s. The PVA layer was soft-baked at $100 \text{ }^\circ\text{C}$ for 1

hour to remove the residual solvent after spin-coating.

To fabricate an organic memristor with a vertical structure, an indium tin oxide (ITO)-patterned substrate (glass for a rigid device and polyethylene naphthalate for a flexible device) was cleaned under ultrasonication in acetone, isopropyl alcohol, and deionized water sequentially for 10 min. Note that the ITO patterns on the substrate acted as inert electrodes of the memristors. Regarding the polymer medium of the devices, PVA, with $M_w = 10000 \text{ gmol}^{-1}$ (or 13000 gmol^{-1}), dissolved in deionized water in 5 wt% (or 4 wt%) was spin-coated on the substrate at a rate of 2000 rpm for 30 s. The PVA layer was then annealed at $100 \text{ }^\circ\text{C}$ for 1 hour. The thickness of the PVA film was about 300 nm. For producing the active electrode, a 50-nm-thick silver layer was thermally evaporated at 1 \AA/s under 10^{-6} Torr. The active area of the devices was $0.5 \times 0.5 \text{ mm}^2$.

Results

We first analyzed the ECM phenomenon for the metallic CF growth in the PVA medium. Three types of planar-structured memristors consisting of PVA insulator with the different M_w s (10000, 23000, and 130000 gmol^{-1}) were fabricated as shown in Figure 1b. Active and inert electrodes were prepared using silver and gold, respectively, and the gap distance between the electrodes was about $5 \text{ }\mu\text{m}$. As shown in Figure S1, in the device with the high M_w of 130000 gmol^{-1} , the resistive switching behaviors were not observed, which is consistent with the previous study (Krishnan et al., 2018). However, the devices with the low M_w of 10000 and 23000 gmol^{-1} clearly showed the resistive switching characteristics (see Figures S2 and S4). In the organic memristors, the ECM phenomenon for resistive switching can be promoted as M_w decreased, because of an increase in the free volumes for ion migration and metallization (Lee et al., 2019a). We measured the current–voltage (I – V) characteristics at six different compliance currents (CCs) (10^{-7} , 5×10^{-7} , 10^{-6} , 5×10^{-6} , 10^{-5} , and 3×10^{-5} A) to explore the ECM phenomenon for resistive switching in the device with $M_w = 10000 \text{ gmol}^{-1}$ (see Figure S2). During the successive voltage sweeps, the CC value was set to be increased sequentially. In all the conditions, the device showed the resistive switching characteristics, and the conductance at the low resistance state (LRS) was larger at higher CCs. However, the LRS of the device was maintained only at relatively high CC conditions (10^{-5} and 3×10^{-5} A). As the CC value increased, the retention performance was enhanced, and the device exhibited a nonvolatile memory behavior in the case when the CC was larger than 10^{-5} A. When the device was operated as a nonvolatile memory, the reversible resistive switching characteristics were also observed (see Figure S3). In typical ECM memristors, the conductance and memory volatility are highly dependent on the CC which governs the CF thickness (Lee et al., 2019a; Hsiung et al., 2010), following the results in Figure S2. Moreover, in the resistive switching device with $M_w = 23000 \text{ gmol}^{-1}$, the nonvolatile memory characteristics were achieved at the relatively low CC conditions, compared to the device with $M_w = 10000 \text{ gmol}^{-1}$. For the organic ECM devices, the lateral diffusion of the CF is governed by the polymer M_w related with the free volume distributions in the medium, and thus, the memory stability is enhanced when M_w is higher (Lee et al., 2020b, 2019a).

Let us discuss the operating principle for the resistive switching in the PVA based memristors. Figure S5 shows the temperature effect on the conductance of the device with $M_w = 10000 \text{ gmol}^{-1}$. The LRS conductance of the device was decreased with the increase in temperature (see Figure S5), which is consistent with the characteristics of the memristors based on the ECM phenomenon (Jang et al., 2016). To clearly elucidate the physical mechanism for the resistive switching in the device, the I – V curves of the device investigated via voltage sweeps with a CC of 10^{-5} A (dark blue curves in Figure S2a) were replotted in a log-log scale, as shown in Figure S6. During the sweeping process, the current flow followed the space charge-limited conduction composed of the regions for the Ohmic, Child’s law, and abrupt conductance increase, consistent with the electrical characteristics of the ECM based nonvolatile memory (Kim et al., 2021a; Sun et al., 2017). This means that the resistive switching behaviors in the device may be governed by the ECM mechanism.

For directly verifying the ECM phenomenon in the device, we carried out the observation of the active surface according to the resistance state, utilizing the field emission electron scanning microscopy (see Figure 1c). With the transition from the high resistance state (HRS) to the LRS, the CFs comprising several branches were formed in the active area of the device. In addition, after the erasing process, the CFs were partially ruptured. The morphology of the CFs in the device at each resistance state was similar to that of other organic ECM memristors (Park et al., 2020c) (Park et al., 2020d, 2021), indicating that the resistive switching characteristics of the PVA based memristors originated from the ECM phenomenon consisting of the electrochemical redox reaction and the ion migration along the polymer medium.

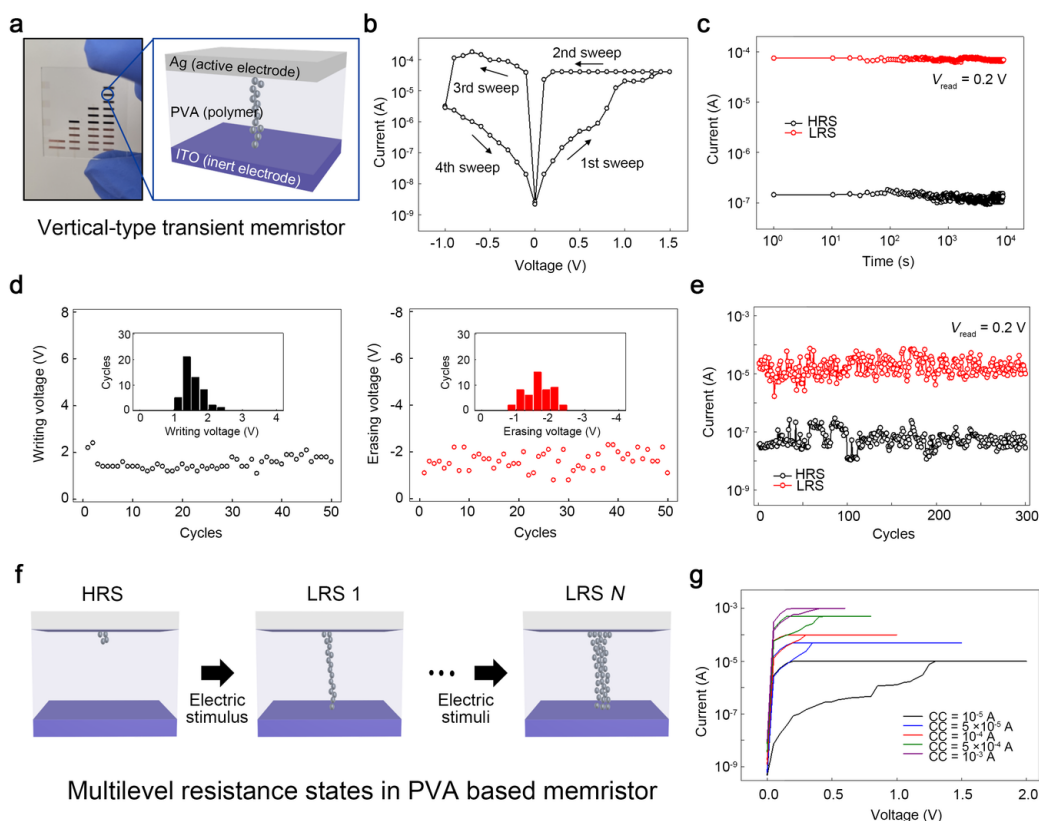


Figure 3: Figure 2. Characterization of the poly (vinyl alcohol) based vertical-type memristor. (a) A photographic image of the vertical-type memristor prepared on a glass substrate. An inset image illustrates the device configuration. (b) Current-voltage characteristics of the device. (c) Memory retention performances of the device. The read voltage (V_{read}) of 0.2 V was used in the measurements. (d) Dispersions of the writing (left) and erasing (right) voltages of the device during the 50 cycles. (e) Electrical durability of the device. A cycle test based on the voltage sweeps was performed, and each resistance state was checked at the V_{read} of 0.2 V. (f) A schematics presenting the multilevel conductances in the device, induced by the control of the CF thickness. (g) Demonstration of the multilevel conductance in the device by tuning the compliance current (CC) condition.

We then developed the PVA based transient memristor with a vertical structure, as shown in **Figure 2a**. The PVA medium with the M_w of 10000 g mol^{-1} was used, and indium tin oxide and silver were utilized as the inert and active electrodes, respectively. The thickness of the polymer medium (PVA) was about 300 nm. Figure 2b exhibits the I - V properties of the device. The measurement was performed at a CC of 3×10^{-5} A to obtain the nonvolatile memory characteristics, and the electroforming process was conducted to trigger the

CF formation (see Figure S7) (Park et al., 2020d, 2021). The device showed the stable nonvolatile memory performances in the bipolar mode, in accordance with the results in Figure S3. The writing and erasing voltages for the device were about 1.4 and -1.0 V, respectively, and the current ratio between the HRS and the LRS was about 10^3 . These operating performances are comparable with those of ECM memristors with inorganic materials (Lee et al., 2020a; Wang et al., 2021). In the previous studies, the hydroxyl groups in the thin films (about 40 nm) of PVA were aligned by an electric field, which led to the memory effect (Lei et al., 2014; Tsai et al., 2013). However, in the cases where the PVA film was relatively thick (about 300 nm), such memory effect was not observed (see Figure S8). This means that the resistive switching in the device is attributed to only the metallic CF growth.

For achieving practical hardware based neural networks, the artificial synapses of the systems should possess the stable nonvolatile and reversible memory characteristics (van de Burgt et al., 2018; Kim et al., 2021a). We performed a retention test for evaluating the memory stability of the developed organic memristor, as shown in Figure 2c. Each resistance state (HRS and LRS) of the device was sustained stably for 10^4 s, at a reading voltage of 0.2 V. Additionally, cycle tests for the device were performed using the repeated voltage sweeps consisting of the writing and erasing processes (see Figures 2d and 2e) to estimate the reproducibility of the operating voltages and the reversibility of the resistive switching. During the 50 cycles, we measured the fluctuations of the writing and erasing voltages, as shown in Figure 2d. The ratio values of the standard deviation to the average for estimating the temporal changes of the writing and erasing voltages were approximately 0.18 and 0.24, respectively. These are comparable with those of the ECM memristors with the conventional structure (Park et al., 2020b; Ding et al., 2018; Chandane et al., 2019). Note that, in the typical ECM memristors, the CF is formed in a random fashion, and it can deteriorate the reproducibility of the switching voltages (Choi et al., 2018). Figure 2e shows the reversibility of the resistive switching in the device. The resistance of the device was stably changed by the switching processes for writing and erasing. From these stable and reversible memory performances, it can be considered that the developed organic memristor is applicable for practical neuromorphic electronics. Figure S9 presents the dispersions of the writing and erasing voltages for ten different cells on a single substrate. Only the small changes were observed in the switching voltages between the cells. Although the device showed the slight fluctuations at the cycle and cell-to-cell uniformity tests, the reproducibility of the switching voltages and the cell uniformity can be facily enhanced by confining the interfacial ion injection (Liu et al., 2010; Lee et al., 2019b).

Another essential feature of memristors for artificial synapses is the multilevel state of the conductance (van de Burgt et al., 2018; Kim et al., 2021a). We controlled the CF thickness by adjusting the CC values at the writing process, as shown in Figure 2f. The multilevel conductance was effectively demonstrated in the device (see Figure 2g), and each conductance state was maintained steadily (see Figure S10). This implies that the developed device can be used for high-density storage systems and complex artificial neural networks. Figure S11 shows the effect of temperature on the conductance of the device at the LRS. The postive resistivity coefficient of the device was estimated to be about 0.0037 K^{-1} , similar to that of silver (about 0.0038 K^{-1}). This implies that the resistive switching of the vertical-type device was governed by the ECM phenomenon for the CF growth (Jang et al., 2016). Note that the ECM memristor is a promising candidate as the highly scalable artificial synapse, because its operation is mainly governed by the localized nanoscale CF (Park et al., 2020d; Choi et al., 2018). As shown in Figure S12, our PVA based memristor showed the stable resistive switching characteristics, irrespective of the cell area.

For the practical applications of neuromorphic systems, the synaptic device should be operated under the pulse condition (Park et al., 2020d, 2021). We additionally investigated the resistive switching of the device in the pulse modes (see Figure S13). The resistance state of the device was effectively controlled by the voltage pulses, and the writing and erasing times were about 5.3 and 5.0 μs , respectively. Typically, in the ECM memristors, the CF growth and the resultant resistive switching are governed by the voltage conditions (Waser et al., 2009; Valov et al., 2011). The switching times of the device can be simply reduced by tuning the voltage amplitude.

To develop a PVA based ECM memristor with mechanical flexibility, we fabricated the vertical-type device

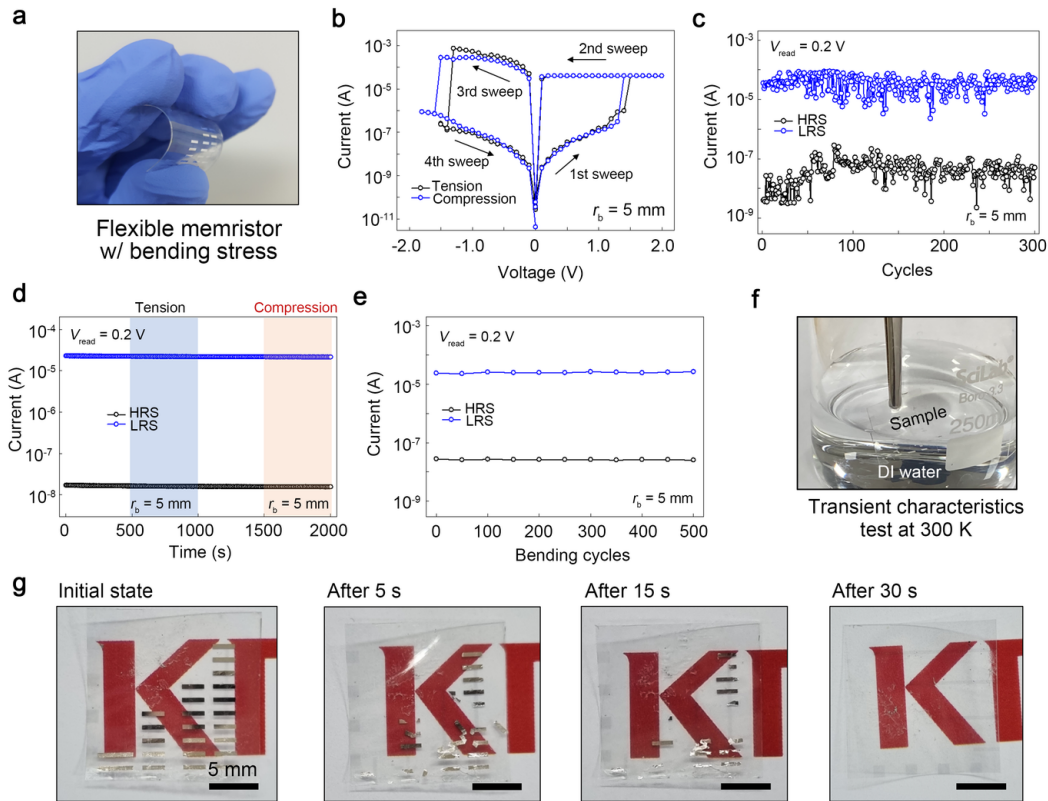


Figure 4: **Figure 3.** Electro-mechanical characteristics of PVA-based flexible memristors. (a) A photographic image of the PVA-based flexible memristor under a mechanical stress with a bending radius (r_b) of 5 mm. (b) Current-voltage characteristics of the flexible device under the bending deformations with $r_b = 5$ mm. (c) Reversible memory performances of the device under the bending stress with $r_b = 5$ mm. (d) Memory retention characteristics of the device investigated under the successive positive and negative bending deformations. The r_b value for each deformation was 5 mm. (e) Mechanical endurance characteristics of the device. (f) A photograph showing the test process for transient characteristics of the device. (g) Photographic images recording the dissolution of the device in deionized water at room temperature (300 K).

with $M_w = 10000$ gmol^{-1} on a flexible substrate of polyethylene naphthalate (PEN), as shown in **Figure 3a**. Figure 3b shows the I - V properties of the flexible memristor at the bending states. Before the measurement, the electroforming process was performed to initiate the CF growth (see Figure S14). We applied the tensile and compressive stresses to the device by conducting the negative and positive bending tests, respectively. The bending radius for the mechanical stresses was 5 mm. The stable resistive switching behaviors which are similar to those in the rigid device (see Figure 3b) were observed in the flexible device at the bending states. Under the positive bending state with a radius of 5 mm, the resistance state of the device was reversibly changed from the HRS to the LRS by the repeated voltage sweeps, as shown in Figure 3c. Furthermore, the device showed the stable resistive switching behaviors under the repeated 5×10^3 pulse cycles (Lanza et al., 2021) (see Figure S15).

To further explore the mechanical durability of the flexible device, we investigated the effect of the repeated mechanical stresses on the memory retention performance of the device (see Figures 3d and 3e). As shown

in Figure 3d, the positive and negative bending processes were performed sequentially in the device, during the memory retention test. The memory states (HRS and LRS) of the device were not deteriorated by the mechanical stresses, which means that the developed memristor can be used as an essential component of flexible neuromorphic systems. Figure 3e shows the results for the bending cycle tests in the device. The device showed a constant conductance at each memory state during the repeated cycles consisting of the positive and negative bending deformations with the same curvatures as those in Figure 3b. Moreover, the device was stably operated as a reversible resistive switching memory after the bending cycle tests (see Figure S16). Considering that mechanical flexibility is a critical requirement for realizing wearable systems (Zhu et al., 2019), the developed memristor with high endurance for bending stresses can be useful in wearable intelligent electronics.

For confirming the transient characteristics of the developed organic memristor, we immersed the device in DI water at a room temperature of 300 K (see Figure 3f) and observed the dissolution state of the device according to the immersion time (see Figure 3g). The device was gradually dissolved in DI water, and completely vanished after 30 s. This transient behavior of the device is superior to those of previously reported transient memory devices (He et al., 2016; Wang et al., 2016a; Wu et al., 2016; Sun et al., 2018; Song et al., 2018; Ji et al., 2018; Xu et al., 2018; Lin et al., 2019). Note that PVA is known to be a carbon-carbon backbone polymer that is biodegradable under both aerobic and anaerobic environments (Zhang et al., 2020). In this regard, the PVA based memristor can be used in a wide range of biodegradable neuromorphic applications.

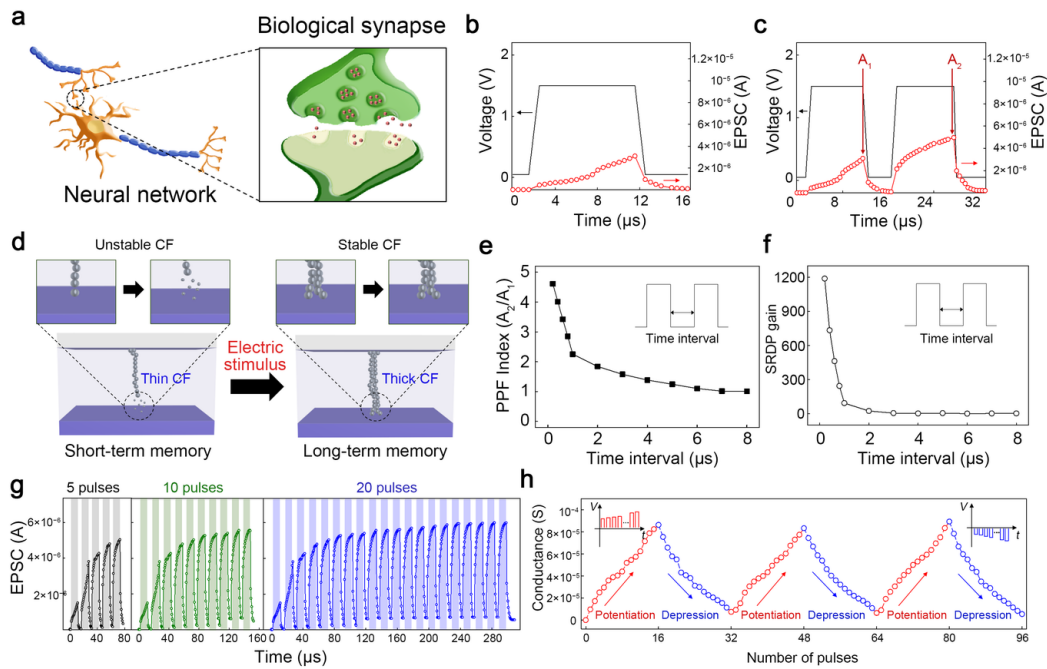


Figure 5: **Figure 4.** Synaptic characteristics of PVA-based flexible memristors. (a) Schematics illustrating biological neural networks consisting of synapses. (b) Excitatory post-synaptic current (EPSC) under electric stimulus. (c) Paired-pulse facilitation (PPF) by two successive voltage pulses (the width and interval for pulses were 10 and 4 μs respectively). (d) Schematics showing a principle for achieving synaptic plasticity in the organic memristor. (e) PPF index as a function of a time interval value between two successive voltage pulses (1.5 V, 10 μs). (f) Spike-rate-dependent plasticity. (g) Spike-number-dependent plasticity under the repeated voltage pulses (1.5 V, 10 μs). (h) Multilevel memory states of the device achieved in the pulse mode.

In realizing the complex artificial neural networks with high energy efficiency, it is important to achieve the synaptic plasticity analogous to the biological counterparts in an artificial synapse (van de Burgt et al., 2018; Bannur et al., 2022; Park et al., 2019) (see **Figure 4a**). The developed flexible memristor exhibited various synaptic functions under electric stimuli. We first measured excitatory post-synaptic current (EPSC) by applying a 10- μ s voltage pulse of 1.5 V as shown in Figure 4b. Under the voltage pulse, the conductance of the device increased and the peak current, EPSC was observed. In addition, the device conductance decreased exponentially after removing the electric stimulus, which is analogous to the STP characteristics of a biological synapse (Salin et al., 1996; Park et al., 2020a). To further verify the STP functions in the flexible memristor, two successive 1.5-V voltage pulses separated by a time interval of 4 μ s were applied to the device (see Figure 4c). The EPSC was larger at the second pulse (A_2) than at the first pulse (A_1), implying the demonstration of PPF, a STP property, in the device. Typically, for the ECM memristors consisting of an insulating layer without any dopant, the lateral diffusion of the metal atoms, and the resultant self-dissolution of the CF are facilitated in the immature filament, which results in the volatile memory characteristics (Lee et al., 2019a; Hua et al., 2019). When the electric stimulus is not sustained sufficiently to grow the CF stably, the developed device exhibits the short-term memory characteristics. In addition, the short-term memory state of the device can be transitioned to the long-term memory state by an additional electric stimulus, before the unstable CF has been disrupted completely (see Figure 4d). As shown in Figure S17, the device showed the volatile memory characteristics under the relatively short pulse condition, however, the device was operated as a non-volatile memory at the longer voltage pulse. Figure 4e shows a PPF index estimated as A_2/A_1 , according to a time interval between the applied voltage pulses. As the interval decreased from 8.0 to 0.2 μ s, the PPF index increased from 1.01 to 4.61, being an indicative of the stable STP properties of the device (Lao et al., 2021; Zhang et al., 2018). Furthermore, we confirmed that the time window of synaptic plasticity can be effectively tuned by the PVA M_w , the diffusive parameter for the CF in the device (Lee et al., 2020b), as shown in Figure S18. As M_w increased, the CF stability and PPF index were enhanced, indicating a slower time window for the synaptic plasticity of the PVA based synapse.

We also investigated SRDP and SNRP, the important spike-dependent learning rules in a brain (Park et al., 2019; Lao et al., 2021), in the flexible device (see Figures 4f and 4g). For SRDP, two consecutive 1.5-V voltage pulses with 10 μ s were applied to the device, and the SRDP gain, a ratio of the increased conductance value to the initial conductance, was measured with different time interval conditions for the applied voltage pulses. Decrease in a time interval from 8.0 to 0.2 μ s, induced an increase in the SRDP gain from 1.05 to 1188.62. Moreover, the EPSC response and the device conductance were effectively tuned through the voltage pulse number (see Figure 4g). With the pulse number, the EPSC value and the device conductance increased. Note that the non-linear increase in the device conductance is attributed to the abrupt growth of the CF, which is similar to the typical ECM memristors (Jang et al., 2019).

For mimicking the reliable memory states of biological synapses, we controlled the device conductance by utilizing the varying electric stimuli, as shown in Figure 4h. In the potentiation process, the voltage pulse with 20 μ s was gradually increased from 1.10 to 1.58 V. For the depression process, the amplitude of the 20- μ s pulse was decreased from -1.00 to -1.48 V. Under such pulse conditions, the device clearly exhibited the multilevel memory states consisting of 16 different conductance levels. It should be noted that, in ECM memristors, voltage pulses with gradually varying amplitudes are ideal electric stimuli for controlling the conductance linearly (Park et al., 2020d). Table S2 shows the electrical performances and synaptic characteristics of the transient memristors previously reported (Hosseini and Lee, 2015; He et al., 2016; Wang et al., 2016a; Wu et al., 2016; Sun et al., 2018; Song et al., 2018; Ji et al., 2018; Xu et al., 2018; Lin et al., 2019; Guo et al., 2020; Sueoka and Zhao, 2022). Although the previous memristors based on various structures exhibited resistive switching characteristics, the synaptic plasticity has not been completely replicated in the devices so far. Based on the optimized synaptic plasticity demonstrated in the developed flexible device, it can be thought that the PVA-based memristor is suitable and ideal for spike-dependent neuromorphic computing applications with high energy efficiency.

For realizing practical neuromorphic systems, parallel computation in synapse arrays is an essential require-

ment (Ielmini and Wong, 2018; Joshi et al., 2020; Yao et al., 2020). To evaluate the potentials of the device for parallel computation with spike-dependent learning process, we prepared the multi-cells of the developed memristors acting as an artificial synapse, as shown in **Figure 5a**. The memristor cells were then trained for logic operators of OR and AND (see Figure 5b), and the consumed energy values for the training and computing processes were analyzed as shown in Figure S19. In training the system, the SRDP characteristics of the cell were used for high energy efficiency and a simple scheme (see Figure S20). For the learning processes of “OR” and “AND”, the developed system consumed approximately 4.28 and 1.01 nJ, respectively. For each logic operation, a single layer consisting of two input neurons and one output neuron was connected by two synapses. In the logic operators, two different binary inputs (V_1 and V_2) with the pulse width of 100 ns were used, and an output current (I_{OR} for OR and I_{AND} for AND) was checked for a logic output. For logic inputs, 0.2 V and 0.002 V were utilized for “1” and “0” respectively, and the measured output current was compared with a threshold current (I_{th}) of 9 μA to estimate the output value. When the output current was higher (or lower) than 9 μA , the logic output was determined as “1” (or “0”). The memristor cells were reliably operated as the logic operators, as shown in Figure 5c. The average operating energy for the “OR” and “AND” logic computing was about 241 fJ, which is superior to that in CMOS systems (Kim et al., 2022). Furthermore, we prepared the synapse array consisting of the 15 different memristor cells to achieve the complex logic operations. To store the letters of “K”, “N”, “U”, “A”, and “I” in the synapse array according to American standard code for information interchange (ASCII) based on the octal numbers, each cell was utilized as a synaptic component with 9 different memory states. The spike-dependent learning processes for the letters (see Figure S21) were effectively performed by consuming about 8.49 nJ, and the computing operation for the stored letters was reliably achieved at a 0.2-V reading voltage with 100 ns, with about 149 fJ (see Figure 5d). This indicates that our memristor can be utilized as an artificial synapse for energy efficient hardware neural networks.

In general, the performances of the artificial neural networks can be evaluated through their recognition capability for several types of pattern images (Feng et al., 2021; Kim et al., 2021b; Shrestha et al., 2021). To confirm the capability of the developed PVA-based memristor for constructing the complex neural network, we conducted the numerical simulation of SPICE for the handwritten digit pattern recognition based on a dataset of the Modified National Institute of Standards and Technology (MNIST) (Kim et al., 2019a; Wang et al., 2020), as shown in Figure 5e. In the simulation, 60000 images for learning and 10000 images for classifying tests were utilized, and the pixel of each image had 256 levels for grayscale. A neural network was simply composed of a single layer, and 784 and 10 neurons were set for the digit images of 28×28 pixels and the classes of the digit images, respectively. The input and output neurons were connected through a single flexible memristor device, as shown in Figure 5f. In the learning processes, the ideal weight distribution calculated in the software system for classifying the digit images for MNIST (see Figure 5g) was converted to the cell conductance in the device arrays. It should be noted that the conductance parameters of the device cell were obtained from the results in Figure 4h. Only positive weight values were utilized to facilitate convert the synaptic weight to the device conductance. Figure 5h shows the conductance distribution of the memristor array after the learning processes for 50 epochs. The ideal synaptic weights consisting of analog memory states were effectively quantized to the 16 levels of the device conductance. For the process of the recognition tests, the 0.1-V input voltage with 100 ns was applied to each cell, and the output current values of bit lines were confirmed. In the neural network based on the developed memristor, the pattern recognition accuracy was about 92 % after training 50 epochs, which is highly close to that of the ideal software system (see Figure 5i). In addition, when the current-sensing resistor of 1 $\text{m}\Omega$ was utilized, the developed hardware neural networks classified digit images by consuming about 255 pJ, which is greatly more efficient than that of the von Neumann counterparts (Shrestha et al., 2021). This implies that the developed PVA-based memristor with biodegradability and mechanical flexibility can be used as a synaptic device in the energy efficient hardware neural networks with high integration density.

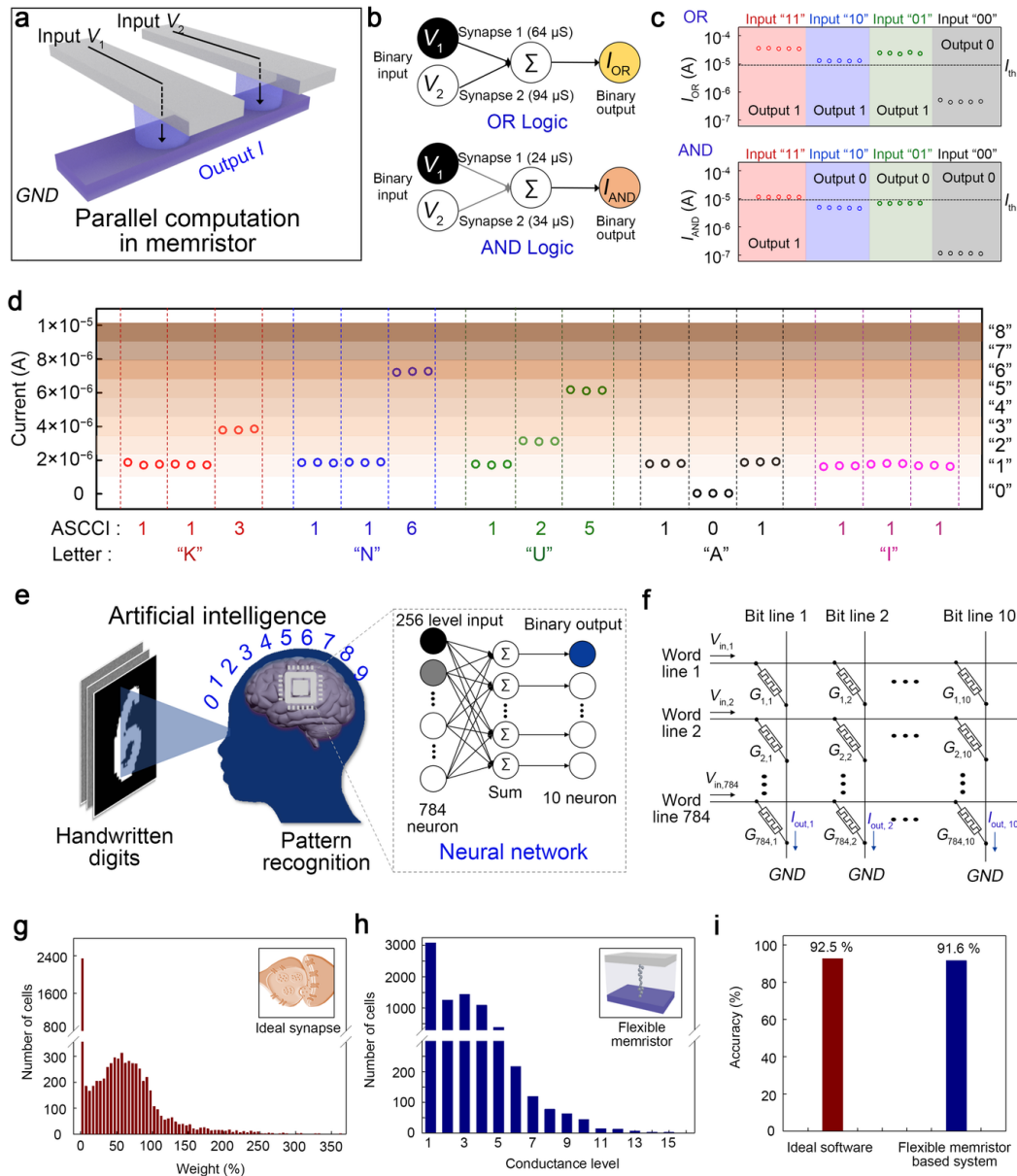


Figure 6: **Figure 5.** An artificial intelligence system based on the developed flexible memristor. (a) A schematic of parallel computation in memristor arrays. (b) Diagram of the trained neural network based on the developed memristor for logic operations of OR and AND. (c) Parallel computation for AND and OR utilizing the developed synapse cells. (d) The letters of “K”, “N”, “U”, “A”, and “I” displayed in the parallel connected synapse cells, according to the ASCII code based on the octal numbers. Each letter was confirmed at a 0.2-V reading voltage with 100 ns. (e) A schematic presenting a configuration of the hardware-based neural network for recognizing the handwritten digit images. (f) A schematic diagram showing the crossbar array of the developed flexible memristor for the neural network. (g) Synaptic weight distribution which was calculated in the ideal software system for recognizing the handwritten digits. (h) Conductance distribution of the developed memristor array after the training process for the recognition of the handwritten digits. (i) The pattern recognition accuracy after the learning processes for 50 epochs in the ideal software system and the hardware-based neural network consisting of the developed flexible memristor.

Conclusion

In conclusion, we demonstrated a biodegradable and flexible polymer based memristor with optimized synaptic plasticity for the spike-dependent learning process. We explored the ECM phenomenon and the resultant CF growth in the pure PVA medium, and analyzed the resistive switching effect of the PVA based memristor. It was found that, in the PVA based memristors, the metallic CF growth and its stability were effectively tuned by the polymer M_w . The developed PVA based memristor was stably operated as a resistive switching memory device, and the multilevel conductance states were effectively achieved by tuning the applied voltage conditions including the CC and the amplitude. The PVA-based memristor prepared on the plastic substrate exhibited the high mechanical flexibility and endurance performances, which is important for practical wearable electronics. Additionally, the developed flexible memristor was also acted as a transient device with highly superior biodegradability due to the high water solubility of the PVA medium. Moreover, the device showed the reliable synaptic characteristics and the applicability as an artificial synapse for the energy efficient neural networks. The simple and complex logic operators were effectively trained in the developed synapse arrays through the spike-dependent learning process with low energy consumption. Furthermore, the intelligent system with high energy efficiency for recognizing the handwritten digits was effectively constructed by utilizing the developed device, and such system exhibited the high pattern recognition accuracy of about 92 % which is close to that of the ideal software neural network. This novel strategy of realizing a transient and flexible synaptic device with the spike-dependent operation would be a fundamental platform for developing eco-friendly smart wearable electronics which are linked to next-generation intelligent systems.

Acknowledgements

S. O. and H. K. contributed equally to this work as the first author. This work was supported by the National Research Foundation of Korea (NRF) under grant funded by the Korea Government (MSIT) (2020R1F1A1075436). This research was supported by National R&D Program through the National Research Foundation of Korea (NRF) funded by Ministry of Science and ICT (2021M3F3A2A03017764). This research was supported by the BK21 FOUR project funded by the Ministry of Education, Korea (4199990113966). This work was supported by the National Research Foundation of Korea (NRF) grant funded by the Korea government (Ministry of Science and ICT) (No. 2021R1C1C2012074). This work was also supported by the National Research Foundation of Korea (NRF) grant funded by the Korea government (MIST) (NRF-2022R1C1C100923511).

Conflict of interest

The authors declare no conflict of interest.

Supporting Information

Supporting Information is available from the Wiley Online Library or from the author.

References

- Hind Ahmed and Ahmed Hashim. Geometry Optimization Optical and Electronic Characteristics of Novel PVA/PEO/SiC Structure for Electronics Applications. *Silicon*, 13(8):2639–2644, jul 2020. doi: 10.1007/s12633-020-00620-0. URL <https://doi.org/10.1007%2Fs12633-020-00620-0>.
- Bharath Bannur, Bhupesh Yadav, and Giridhar U. Kulkarni. Second-Order Conditioning Emulated in an Artificial Synaptic Network. *ACS Applied Electronic Materials*, 4(4):1552–1557, mar 2022. doi: 10.1021/acsaelm.1c01237. URL <https://doi.org/10.1021%2Facsaelm.1c01237>.
- Pratiksha T. Chandane, Tukaram D. Dongale, Prashant B. Patil, and Arpita P. Tiwari. Organic resistive switching device based on cellulose-gelatine microcomposite fibers. *Journal of Materials Science: Materials in Electronics*, 30(24):21288–21296, nov 2019. doi: 10.1007/s10854-019-02503-6. URL <https://doi.org/10.1007%2Fs10854-019-02503-6>.
- Shinhyun Choi, Scott H. Tan, Zefan Li, Yunjo Kim, Chanyeol Choi, Pai-Yu Chen, Hanwool Yeon, Shimeng Yu, and Jeehwan Kim. SiGe epitaxial memory for neuromorphic computing with reproducible high performance based on engineered dislocations. *Nature Materials*, 17(4):335–340, jan 2018. doi: 10.1038/s41563-017-0001-5. URL <https://doi.org/10.1038%2Fs41563-017-0001-5>.
- Wentao Ding, Ye Tao, Xuhong Li, Ya Lin, Zhongqiang Wang, Haiyang Xu, Xiaoning Zhao, Weizhen Liu, Jiangang Ma, and Yichun Liu. Graphite Microislands Prepared for Reliability Improvement of Amorphous Carbon Based Resistive Switching Memory. *physica status solidi (RRL) - Rapid Research Letters*, 12(10):1800285, jul 2018. doi: 10.1002/pssr.201800285. URL <https://doi.org/10.1002%2Fpssr.201800285>.
- Andrea Dorigato and Alessandro Pegoretti. Biodegradable single-polymer composites from polyvinyl alcohol. *Colloid and Polymer Science*, 290(4):359–370, dec 2011. doi: 10.1007/s00396-011-2556-z. URL <https://doi.org/10.1007%2Fs00396-011-2556-z>.
- Xuwei Feng, Yida Li, Lin Wang, Shuai Chen, Zhi Gen Yu, Wee Chong Tan, Nasiruddin Macadam, Guohua Hu, Li Huang, Li Chen, Xiao Gong, Dongzhi Chi, Tawfique Hasan, Aaron Voon-Yew Thean, Yong-Wei Zhang, and Kah-Wee Ang. A Fully Printed Flexible MoS₂ Memristive Artificial Synapse with Femtojoule Switching Energy. *Advanced Electronic Materials*, 5(12):1900740, sep 2019. doi: 10.1002/aelm.201900740. URL <https://doi.org/10.1002%2Faelm.201900740>.
- Xuwei Feng, Sifan Li, Swee Liang Wong, Shiwun Tong, Li Chen, Panpan Zhang, Lingfei Wang, Xuanyao Fong, Dongzhi Chi, and Kah-Wee Ang. Self-Selective Multi-Terminal Memtransistor Crossbar Array for In-Memory Computing. *ACS Nano*, 15(1):1764–1774, jan 2021. doi: 10.1021/acsnano.0c09441. URL <https://doi.org/10.1021%2Facs.nano.0c09441>.
- Kun Kelvin Fu, Zhengyang Wang, Jiaqi Dai, Marcus Carter, and Liangbing Hu. Transient Electronics: Materials and Devices. *Chemistry of Materials*, 28(11):3527–3539, may 2016. doi: 10.1021/acs.chemmater.5b04931. URL <https://doi.org/10.1021%2Facs.chemmater.5b04931>.
- Yang Gao, Ying Zhang, Xu Wang, Kyoseung Sim, Jingshen Liu, Ji Chen, Xue Feng, Hangxun Xu, and Cunjiang Yu. Moisture-triggered physically transient electronics. *Science Advances*, 3(9), sep 2017. doi: 10.1126/sciadv.1701222. URL <https://doi.org/10.1126%2Fsciadv.1701222>.
- Yuanyang Guo, Wei Hu, Fanju Zeng, Changgeng Zhang, Yao Peng, and Yongcai Guo. Ultrafast degradable resistive switching memory based on -lactose thin films. *Organic Electronics*, 83:105750, aug 2020. doi: 10.1016/j.orgel.2020.105750. URL <https://doi.org/10.1016%2Fj.orgel.2020.105750>.

- Xingli He, Jian Zhang, Wenbo Wang, Weipeng Xuan, Xiaozhi Wang, Qilong Zhang, Charles G. Smith, and Jikui Luo. Transient Resistive Switching Devices Made from Egg Albumen Dielectrics and Dissolvable Electrodes. *ACS Applied Materials & Interfaces*, 8(17):10954–10960, apr 2016. doi: 10.1021/acsami.5b10414. URL <https://doi.org/10.1021%2Facsami.5b10414>.
- Jehova Jire L. Hmar. Flexible resistive switching bistable memory devices using ZnO nanoparticles embedded in polyvinyl alcohol (PVA) matrix and poly(3,4-ethylenedioxythiophene) polystyrene sulfonate (PEDOT:PSS). *RSC Advances*, 8(36):20423–20433, 2018. doi: 10.1039/c8ra04582h. URL <https://doi.org/10.1039%2Fc8ra04582h>.
- Niloufar Raeis Hosseini and Jang-Sik Lee. Biocompatible and Flexible Chitosan-Based Resistive Switching Memory with Magnesium Electrodes. *Advanced Functional Materials*, 25(35):5586–5592, aug 2015. doi: 10.1002/adfm.201502592. URL <https://doi.org/10.1002%2Fadfm.201502592>.
- Chang-Po Hsiung, Hsin-Wei Liao, Jon-Yiew Gan, Tai-Bo Wu, Jenn-Chang Hwang, Frederick Chen, and Ming-Jinn Tsai. Formation and Instability of Silver Nanofilament in Ag-Based Programmable Metallization Cells. *ACS Nano*, 4(9):5414–5420, aug 2010. doi: 10.1021/nn1010667. URL <https://doi.org/10.1021%2Fnn1010667>.
- Qilin Hua, Huaqiang Wu, Bin Gao, Meiran Zhao, Yujia Li, Xinyi Li, Xiang Hou, Meng-Fan (Marvin) Chang, Peng Zhou, and He Qian. A Threshold Switching Selector Based on Highly Ordered Ag Nanodots for X-Point Memory Applications. *Advanced Science*, 6(10):1900024, apr 2019. doi: 10.1002/advs.201900024. URL <https://doi.org/10.1002%2Fadvs.201900024>.
- Daniele Ielmini and H.-S. Philip Wong. In-memory computing with resistive switching devices. *Nature Electronics*, 1(6):333–343, jun 2018. doi: 10.1038/s41928-018-0092-2. URL <https://doi.org/10.1038%2Fs41928-018-0092-2>.
- Byung Chul Jang, Hyejeong Seong, Sung Kyu Kim, Jong Yun Kim, Beom Jun Koo, Junhwan Choi, Sang Yoon Yang, Sung Gap Im, and Sung-Yool Choi. Flexible Nonvolatile Polymer Memory Array on Plastic Substrate via Initiated Chemical Vapor Deposition. *ACS Applied Materials & Interfaces*, 8(20):12951–12958, may 2016. doi: 10.1021/acsami.6b01937. URL <https://doi.org/10.1021%2Facsami.6b01937>.
- Byung Chul Jang, Sungkyu Kim, Sang Yoon Yang, Jihun Park, Jun-Hwe Cha, Jungyeop Oh, Junhwan Choi, Sung Gap Im, Vinayak P. Dravid, and Sung-Yool Choi. Polymer Analog Memristive Synapse with Atomic-Scale Conductive Filament for Flexible Neuromorphic Computing System. *Nano Letters*, 19(2):839–849, jan 2019. doi: 10.1021/acs.nanolett.8b04023. URL <https://doi.org/10.1021%2Facs.nanolett.8b04023>.
- Xinglong Ji, Li Song, Shuai Zhong, Yu Jiang, Kian Guan Lim, Chao Wang, and Rong Zhao. Biodegradable and Flexible Resistive Memory for Transient Electronics. *The Journal of Physical Chemistry C*, 122(29):16909–16915, jun 2018. doi: 10.1021/acs.jpcc.8b03075. URL <https://doi.org/10.1021%2Facs.jpcc.8b03075>.
- Vinay Joshi, Manuel Le Gallo, Simon Haefeli, Irem Boybat, S. R. Nandakumar, Christophe Piveteau, Martino Dazzi, Bipin Rajendran, Abu Sebastian, and Evangelos Eleftheriou. Accurate deep neural network inference using computational phase-change memory. *Nature Communications*, 11(1), may 2020. doi: 10.1038/s41467-020-16108-9. URL <https://doi.org/10.1038%2Fs41467-020-16108-9>.
- Min-Hwi Kim, Hea-Lim Park, Min-Hoi Kim, Jaewon Jang, Jin-Hyuk Bae, In Man Kang, and Sin-Hyung Lee. Fluoropolymer-based organic memristor with multifunctionality for flexible neural network system. *npj Flexible Electronics*, 5(1), dec 2021a. doi: 10.1038/s41528-021-00132-w. URL <https://doi.org/10.1038%2Fs41528-021-00132-w>.
- Seong Eun Kim, Min-Hwi Kim, Jisu Jang, Hyungjin Kim, Sungjun Kim, Jaewon Jang, Jin-Hyuk Bae, In Man Kang, and Sin-Hyung Lee. Systematic Engineering of Metal Ion Injection in Memristors for

Complex Neuromorphic Computing with High Energy Efficiency. *Advanced Intelligent Systems*, 4(9): 2200110, jun 2022. doi: 10.1002/aisy.202200110. URL <https://doi.org/10.1002%2Faisy.202200110>.

Sungjun Kim, Jia Chen, Ying-Chen Chen, Min-Hwi Kim, Hyungjin Kim, Min-Woo Kwon, Sungmin Hwang, Muhammad Ismail, Yi Li, Xiang-Shui Miao, Yao-Feng Chang, and Byung-Gook Park. Neuronal dynamics in HfO₂/AlO_x-based homeothermic synaptic memristors with low-power and homogeneous resistive switching. *Nanoscale*, 11(1):237–245, 2019a. doi: 10.1039/c8nr06694a. URL <https://doi.org/10.1039%2Fc8nr06694a>.

Sungjun Kim, Keun Heo, Sunghun Lee, Seunghwan Seo, Hyeongjun Kim, Jeongick Cho, Hyunkyoo Lee, Kyeong-Bae Lee, and Jin-Hong Park. Ferroelectric polymer-based artificial synapse for neuromorphic computing. *Nanoscale Horizons*, 6(2):139–147, 2021b. doi: 10.1039/d0nh00559b. URL <https://doi.org/10.1039%2Fd0nh00559b>.

Taeheon Kim, Dong-Kyun Kim, Jongtae Kim, and James J Pak. Resistive switching behaviour of multi-stacked PVA/graphene oxide + PVA composite/PVA insulating layer-based RRAM devices. *Semiconductor Science and Technology*, 34(6):065006, may 2019b. doi: 10.1088/1361-6641/ab1403. URL <https://doi.org/10.1088%2F1361-6641%2Fab1403>.

Karthik Krishnan, Masakazu Aono, and Tohru Tsuruoka. Thermally stable resistive switching of a polyvinyl alcohol-based atomic switch. *Journal of Materials Chemistry C*, 6(24):6460–6464, 2018. doi: 10.1039/c8tc01809j. URL <https://doi.org/10.1039%2Fc8tc01809j>.

Mario Lanza, Rainer Waser, Daniele Ielmini, J. Joshua Yang, Ludovic Goux, Jordi Suñe, Anthony Joseph Kenyon, Adnan Mehonic, Sabina Spiga, Vikas Rana, Stefan Wiefels, Stephan Menzel, Ilia Valov, Marco A. Villena, Enrique Miranda, Xu Jing, Francesca Campabadal, Mireia B. Gonzalez, Fernando Aguirre, Felix Palumbo, Kaichen Zhu, Juan Bautista Roldan, Francesco Maria Puglisi, Luca Larcher, Tuo-Hung Hou, Themis Prodromakis, Yuchao Yang, Peng Huang, Tianqing Wan, Yang Chai, Kin Leong Pey, Nagarajan Raghavan, Salvador Dueñas, Tao Wang, Qiangfei Xia, and Sebastian Pazos. Standards for the Characterization of Endurance in Resistive Switching Devices. *ACS Nano*, 15(11):17214–17231, nov 2021. doi: 10.1021/acsnano.1c06980. URL <https://doi.org/10.1021%2Facs.nano.1c06980>.

Jie Lao, Wen Xu, Chunli Jiang, Ni Zhong, Bobo Tian, Hechun Lin, Chunhua Luo, Jadranka Travas-sejdic, Hui Peng, and Chun-Gang Duan. An air-stable artificial synapse based on a lead-free double perovskite Cs₂AgBiBr₆ film for neuromorphic computing. *Journal of Materials Chemistry C*, 9(17): 5706–5712, 2021. doi: 10.1039/d1tc00655j. URL <https://doi.org/10.1039%2Fd1tc00655j>.

Jinju Lee, Ji-Ho Ryu, Boram Kim, Fayyaz Hussain, Chandreswar Mahata, Eunjin Sim, Muhammad Ismail, Yawar Abbas, Haider Abbas, Dong Keun Lee, Min-Hwi Kim, Yoon Kim, Changhwan Choi, Byung-Gook Park, and Sungjun Kim. Synaptic Characteristics of Amorphous Boron Nitride-Based Memristors on a Highly Doped Silicon Substrate for Neuromorphic Engineering. *ACS Applied Materials & Interfaces*, 12(30):33908–33916, jul 2020a. doi: 10.1021/acsaami.0c07867. URL <https://doi.org/10.1021%2Facsami.0c07867>.

Sin-Hyung Lee, Hea-Lim Park, Chang-Min Keum, In-Ho Lee, Min-Hoi Kim, and Sin-Doo Lee. Organic Flexible Memristor with Reduced Operating Voltage and High Stability by Interfacial Control of Conductive Filament Growth. *physica status solidi (RRL) – Rapid Research Letters*, 13(6):1900044, feb 2019a. doi: 10.1002/pssr.201900044. URL <https://doi.org/10.1002%2Fpssr.201900044>.

Sin-Hyung Lee, Hea-Lim Park, Min-Hoi Kim, Sujie Kang, and Sin-Doo Lee. Interfacial Triggering of Conductive Filament Growth in Organic Flexible Memristor for High Reliability and Uniformity. *ACS Applied Materials & Interfaces*, 11(33):30108–30115, jul 2019b. doi: 10.1021/acsaami.9b10491. URL <https://doi.org/10.1021%2Facsami.9b10491>.

Sin-Hyung Lee, Hea-Lim Park, Min-Hoi Kim, Min-Hwi Kim, Byung-Gook Park, and Sin-Doo Lee. Realization of Biomimetic Synaptic Functions in a One-Cell Organic Resistive Switching Device Using the

- Diffusive Parameter of Conductive Filaments. *ACS Applied Materials & Interfaces*, 12(46):51719–51728, nov 2020b. doi: 10.1021/acsami.0c15519. URL <https://doi.org/10.1021%2Facsami.0c15519>.
- Yan Lei, Yi Liu, Yidong Xia, Xu Gao, Bo Xu, Suidong Wang, Jiang Yin, and Zhiguo Liu. Memristive learning and memory functions in polyvinyl alcohol polymer memristors. *AIP Advances*, 4(7):077105, jul 2014. doi: 10.1063/1.4887010. URL <https://doi.org/10.1063%2F1.4887010>.
- Steven Lequeux, Joao Sampaio, Vincent Cros, Kay Yakushiji, Akio Fukushima, Rie Matsumoto, Hitoshi Kubota, Shinji Yuasa, and Julie Grollier. A magnetic synapse: multilevel spin-torque memristor with perpendicular anisotropy. *Scientific Reports*, 6(1), aug 2016. doi: 10.1038/srep31510. URL <https://doi.org/10.1038%2Fsrep31510>.
- Qiqi Lin, Shilei Hao, Wei Hu, Ming Wang, Zhigang Zang, Linna Zhu, Juan Du, and Xiaosheng Tang. Human hair keratin for physically transient resistive switching memory devices. *Journal of Materials Chemistry C*, 7(11):3315–3321, 2019. doi: 10.1039/c8tc05334k. URL <https://doi.org/10.1039%2F8tc05334k>.
- Qi Liu, Shibing Long, Hangbing Lv, Wei Wang, Jiebin Niu, Zongliang Huo, Juning Chen, and Ming Liu. Controllable Growth of Nanoscale Conductive Filaments in Solid-Electrolyte-Based ReRAM by Using a Metal Nanocrystal Covered Bottom Electrode. *ACS Nano*, 4(10):6162–6168, sep 2010. doi: 10.1021/nn1017582. URL <https://doi.org/10.1021%2Fnn1017582>.
- Pei-Pei Lu, Jian-Xin Shen, Da-Shan Shang, and Young Sun. Nonvolatile Memory and Artificial Synapse Based on the Cu/P(VDF-TrFE)/Ni Organic Memtranstor. *ACS Applied Materials & Interfaces*, 12(4): 4673–4677, jan 2020. doi: 10.1021/acsami.9b19510. URL <https://doi.org/10.1021%2Facsami.9b19510>.
- Hai Hung Nguyen, Hanh Kieu Thi Ta, Sungkyun Park, Thang Bach Phan, and Ngoc Kim Pham. Resistive switching effect and magnetic properties of iron oxide nanoparticles embedded-polyvinyl alcohol film. *RSC Advances*, 10(22):12900–12907, 2020. doi: 10.1039/c9ra10101b. URL <https://doi.org/10.1039%2F9ra10101b>.
- Hea-Lim Park and Tae-Woo Lee. Organic and perovskite memristors for neuromorphic computing. *Organic Electronics*, 98:106301, nov 2021. doi: 10.1016/j.orgel.2021.106301. URL <https://doi.org/10.1016%2Fj.orgel.2021.106301>.
- Hea-Lim Park, Yeongjun Lee, Naryung Kim, Dae-Gyo Seo, Gyeong-Tak Go, and Tae-Woo Lee. Flexible Neuromorphic Electronics for Computing Soft Robotics, and Neuroprosthetics. *Advanced Materials*, 32(15): 1903558, sep 2019. doi: 10.1002/adma.201903558. URL <https://doi.org/10.1002%2Fadma.201903558>.
- Hea-Lim Park, Haeju Kim, Donggyu Lim, Huanyu Zhou, Young-Hoon Kim, Yeongjun Lee, Sungjin Park, and Tae-Woo Lee. Retina-Inspired Carbon Nitride-Based Photonic Synapses for Selective Detection of UV Light. *Advanced Materials*, 32(11):1906899, jan 2020a. doi: 10.1002/adma.201906899. URL <https://doi.org/10.1002%2Fadma.201906899>.
- Hea-Lim Park, Min-Hoi Kim, and Sin-Hyung Lee. Introduction of Interfacial Load Polymeric Layer to Organic Flexible Memristor for Regulating Conductive Filament Growth. *Advanced Electronic Materials*, 6(10):2000582, sep 2020b. doi: 10.1002/aelm.202000582. URL <https://doi.org/10.1002%2Faelm.202000582>.
- Hea-Lim Park, Min-Hoi Kim, and Sin-Hyung Lee. Control of conductive filament growth in flexible organic memristor by polymer alignment. *Organic Electronics*, 87:105927, dec 2020c. doi: 10.1016/j.orgel.2020.105927. URL <https://doi.org/10.1016%2Fj.orgel.2020.105927>.
- Hea-Lim Park, Min-Hwi Kim, Min-Hoi Kim, and Sin-Hyung Lee. Reliable organic memristors for neuromorphic computing by predefining a localized ion-migration path in crosslinkable polymer. *Nanoscale*, 12(44):22502–22510, 2020d. doi: 10.1039/d0nr06964g. URL <https://doi.org/10.1039%2Fd0nr06964g>.
- Hea-Lim Park, Min-Hwi Kim, Hyungjin Kim, and Sin-Hyung Lee. Self-Selective Organic Memristor by Engineered Conductive Nanofilament Diffusion for Realization of Practical Neuromorphic System.

- Advanced Electronic Materials*, 7(8):2100299, jun 2021. doi: 10.1002/aelm.202100299. URL <https://doi.org/10.1002%2Faelm.202100299>.
- Youngjun Park and Jang-Sik Lee. Bifunctional Silver-Doped ZnO for Reliable and Stable Organic–Inorganic Hybrid Perovskite Memory. *ACS Applied Materials & Interfaces*, 13(1):1021–1026, dec 2020. doi: 10.1021/acsami.0c18038. URL <https://doi.org/10.1021%2Facsami.0c18038>.
- Niloufar Raeis-Hosseini, Youngjun Park, and Jang-Sik Lee. Flexible Artificial Synaptic Devices Based on Collagen from Fish Protein with Spike-Timing-Dependent Plasticity. *Advanced Functional Materials*, 28(31):1800553, jun 2018. doi: 10.1002/adfm.201800553. URL <https://doi.org/10.1002%2Fadfm.201800553>.
- Paul A. Salin, Massimo Scanziani, Robert C. Malenka, and Roger A. Nicoll. Distinct short-term plasticity at two excitatory synapses in the hippocampus. *Proceedings of the National Academy of Sciences*, 93(23):13304–13309, nov 1996. doi: 10.1073/pnas.93.23.13304. URL <https://doi.org/10.1073%2Fpnas.93.23.13304>.
- Syed Ghazi Sarwat, Benedikt Kersting, Timoleon Moraitis, Vara Prasad Jonnalagadda, and Abu Sebastian. Phase-change memtransistive synapses for mixed-plasticity neural computations. *Nature Nanotechnology*, 17(5):507–513, mar 2022. doi: 10.1038/s41565-022-01095-3. URL <https://doi.org/10.1038%2Fs41565-022-01095-3>.
- Amar Shrestha, Haowen Fang, Daniel Patrick Rider, Zaidao Mei, and Qinru Qiu. In-Hardware Learning of Multilayer Spiking Neural Networks on a Neuromorphic Processor. In *2021 58th ACM/IEEE Design Automation Conference (DAC)*. IEEE, dec 2021. doi: 10.1109/dac18074.2021.9586323. URL <https://doi.org/10.1109%2Fdac18074.2021.9586323>.
- Fang Song, Hong Wang, Jing Sun, Haixia Gao, Shiwei Wu, Mei Yang, Xiaohua Ma, and Yue Hao. ZnO-Based Physically Transient and Bioresorbable Memory on Silk Protein. *IEEE Electron Device Letters*, 39(1):31–34, jan 2018. doi: 10.1109/led.2017.2774842. URL <https://doi.org/10.1109%2Fled.2017.2774842>.
- Brandon Sueoka and Feng Zhao. Memristive synaptic device based on a natural organic material—honey for spiking neural network in biodegradable neuromorphic systems. *Journal of Physics D: Applied Physics*, 55(22):225105, mar 2022. doi: 10.1088/1361-6463/ac585b. URL <https://doi.org/10.1088%2F1361-6463%2Fac585b>.
- Jing Sun, Hong Wang, Fang Song, Zhan Wang, Bingjie Dang, Mei Yang, Haixia Gao, Xiaohua Ma, and Yue Hao. Physically Transient Threshold Switching Device Based on Magnesium Oxide for Security Application. *Small*, 14(27):1800945, may 2018. doi: 10.1002/smll.201800945. URL <https://doi.org/10.1002%2Fsmll.201800945>.
- Yanmei Sun, Nian He, Dianzhong Wen, and Fengyun Sun. The nonvolatile resistive switching memristor with Co-Ni layered double hydroxide hybrid nanosheets and its application as a artificial synapse. *Applied Surface Science*, 564:150452, oct 2021. doi: 10.1016/j.apsusc.2021.150452. URL <https://doi.org/10.1016%2Fj.apsusc.2021.150452>.
- Yiming Sun, Cheng Song, Jun Yin, Xianzhe Chen, Qin Wan, Fei Zeng, and Feng Pan. Guiding the Growth of a Conductive Filament by Nanoindentation To Improve Resistive Switching. *ACS Applied Materials & Interfaces*, 9(39):34064–34070, sep 2017. doi: 10.1021/acsami.7b09710. URL <https://doi.org/10.1021%2Facsami.7b09710>.
- Tzung-Da Tsai, Jer-Wei Chang, Ten-Chin Wen, and Tzung-Fang Guo. Manipulating the Hysteresis in Poly(vinyl alcohol)-Dielectric Organic Field-Effect Transistors Toward Memory Elements. *Advanced Functional Materials*, 23(34):4206–4214, mar 2013. doi: 10.1002/adfm.201203694. URL <https://doi.org/10.1002%2Fadfm.201203694>.
- Iliia Valov, Rainer Waser, John R Jameson, and Michael N Kozicki. Electrochemical metallization memo-

ries—fundamentals applications, prospects. *Nanotechnology*, 22(25):254003, may 2011. doi: 10.1088/0957-4484/22/25/254003. URL <https://doi.org/10.1088%2F0957-4484%2F22%2F25%2F254003>.

Yoeri van de Burgt, Armantas Melianas, Scott Tom Keene, George Malliaras, and Alberto Salleo. Organic electronics for neuromorphic computing. *Nature Electronics*, 1(7):386–397, jul 2018. doi: 10.1038/s41928-018-0103-3. URL <https://doi.org/10.1038%2Fs41928-018-0103-3>.

Hong Wang, Bowen Zhu, Xiaohua Ma, Yue Hao, and Xiaodong Chen. Physically Transient Resistive Switching Memory Based on Silk Protein. *Small*, 12(20):2715–2719, mar 2016a. doi: 10.1002/smll.201502906. URL <https://doi.org/10.1002%2Fsmll.201502906>.

Xiangdong Wang, Xiaoyu Wang, Menghan Pi, and Rong Ran. High-strength highly conductive and woven organic hydrogel fibers for flexible electronics. *Chemical Engineering Journal*, 428:131172, jan 2022. doi: 10.1016/j.cej.2021.131172. URL <https://doi.org/10.1016%2Fj.cej.2021.131172>.

Zhongrui Wang, Saamil Joshi, Sergey E. Savel'ev, Hao Jiang, Rivu Midya, Peng Lin, Miao Hu, Ning Ge, John Paul Strachan, Zhiyong Li, Qing Wu, Mark Barnell, Geng-Lin Li, Huolin L. Xin, R. Stanley Williams, Qiangfei Xia, and J. Joshua Yang. Memristors with diffusive dynamics as synaptic emulators for neuromorphic computing. *Nature Materials*, 16(1):101–108, sep 2016b. doi: 10.1038/nmat4756. URL <https://doi.org/10.1038%2Fnmat4756>.

Ziyi Wang, Bo Sun, Haibo Ye, Zhiyong Liu, Guanglan Liao, and Tielin Shi. Annealed AlOx film with enhanced performance for bipolar resistive switching memory. *Applied Surface Science*, 546:149094, apr 2021. doi: 10.1016/j.apsusc.2021.149094. URL <https://doi.org/10.1016%2Fj.apsusc.2021.149094>.

Zongwei Wang, Qilin Zheng, Jian Kang, Zhizhen Yu, Guofang Zhong, Yaotian Ling, Lin Bao, Shengyu Bao, Guandong Bai, Shan Zheng, Yimao Cai, John Robertson, and Ru Huang. Self-Activation Neural Network Based on Self-Selective Memory Device With Rectified Multilevel States. *IEEE Transactions on Electron Devices*, 67(10):4166–4171, oct 2020. doi: 10.1109/ted.2020.3014566. URL <https://doi.org/10.1109%2Fted.2020.3014566>.

Rainer Waser, Regina Dittmann, Georgi Staikov, and Kristof Szot. Redox-Based Resistive Switching Memories - Nanoionic Mechanisms Prospects, and Challenges. *Advanced Materials*, 21(25-26):2632–2663, jul 2009. doi: 10.1002/adma.200900375. URL <https://doi.org/10.1002%2Fadma.200900375>.

Kyung Seok Woo, Jaehyun Kim, Janguk Han, Jin Myung Choi, Woohyun Kim, and Cheol Seong Hwang. A High-Speed True Random Number Generator Based on a Cu sub ix/i /sub Te sub 1- ix/i /sub Diffusive Memristor. *Advanced Intelligent Systems*, 3(7):2100062, jun 2021. doi: 10.1002/aisy.202100062. URL <https://doi.org/10.1002%2Faisy.202100062>.

Shiwei Wu, Hong Wang, Jing Sun, Fang Song, Zhan Wang, Mei Yang, He Xi, Yong Xie, Haixia Gao, Jigang Ma, Xiaohua Ma, and Yue Hao. Dissolvable and biodegradable resistive switching memory based on magnesium oxide. *IEEE Electron Device Letters*, pages 1–1, 2016. doi: 10.1109/led.2016.2585665. URL <https://doi.org/10.1109%2Fled.2016.2585665>.

Jiaqi Xu, Xiaoning Zhao, Zhongqiang Wang, Haiyang Xu, Junli Hu, Jiangang Ma, and Yichun Liu. Biodegradable Natural Pectin-Based Flexible Multilevel Resistive Switching Memory for Transient Electronics. *Small*, 15(4):1803970, nov 2018. doi: 10.1002/smll.201803970. URL <https://doi.org/10.1002%2Fsmll.201803970>.

Peng Yao, Huaqiang Wu, Bin Gao, Jianshi Tang, Qingtian Zhang, Wenqiang Zhang, J. Joshua Yang, and He Qian. Fully hardware-implemented memristor convolutional neural network. *Nature*, 577(7792):641–646, jan 2020. doi: 10.1038/s41586-020-1942-4. URL <https://doi.org/10.1038%2Fs41586-020-1942-4>.

Shi-Rui Zhang, Li Zhou, Jing-Yu Mao, Yi Ren, Jia-Qin Yang, Guang-Hu Yang, Xin Zhu, Su-Ting Han, Vellaisamy A. L. Roy, and Ye Zhou. Artificial Synapse Emulated by Charge Trapping-Based Resistive

Switching Device. *Advanced Materials Technologies*, 4(2):1800342, oct 2018. doi: 10.1002/admt.201800342. URL <https://doi.org/10.1002%2Fadmt.201800342>.

Ziwei Zhang, Chunhui Du, Haoxuan Jiao, and Min Zhang. Polyvinyl Alcohol/SiO₂ Hybrid Dielectric for Transparent Flexible/Stretchable All-Carbon-Nanotube Thin-Film-Transistor Integration. *Advanced Electronic Materials*, 6(5):1901133, mar 2020. doi: 10.1002/aem.201901133. URL <https://doi.org/10.1002%2Faelm.201901133>.

Chuang Zhu, Evelyn Chalmers, Liming Chen, Yuqi Wang, Ben Bin Xu, Yi Li, and Xuqing Liu. A Nature-Inspired Flexible Substrate Strategy for Future Wearable Electronics. *Small*, 15(35):1902440, jun 2019. doi: 10.1002/sml.201902440. URL <https://doi.org/10.1002%2Fsml.201902440>.